Prediction of Chiral Discrimination by β-Cyclodextrins Using Grid-based Monte Carlo Docking Simulations

Youngjin Choi,[1] Dong Wook Kim,[2] Hyungwoo Park,[3] Suntae Hwang,[4] Karpjoo Jeong,[5,6,*] and Seunho Jung[1,6,*]

[1]*Department of Microbial Engineering &* [6]*Department of Advanced Technology Fusion, Bio/Molecular Informatics Center, Konkuk University, Seoul 143-701, Korea.* *E-mail: shjung@konkuk.ac.kr*
[2]*Electronics and Telecommunications Research Institute, Daejeon 305-350, Korea*
[3]*Korea Institute of Science and Technology Information, Daejeon 305-333, Korea*
[4]*Department of Computer Science, Kookmin University, Seoul 136-702, Korea*
[5]*College of Information and Communication, Konkuk University, Seoul 143-701, Korea.* *E-mail: jeongk@konkuk.ac.kr*
Received January 31, 2005

An efficiency of Monte Carlo (MC) docking simulations was examined for the prediction of chiral discrimination by cyclodextrins. Docking simulations were performed with various computational parameters for the chiral discrimination of a series of 17 enantiomers by β-cyclodextrin (β-CD) or by 6-amino-6-deoxy-β-cyclodextrin (am-β-CD). A total of 30 sets of enantiomeric complexes were tested to find the optimal simulation parameters for accurate predictions. Rigid-body MC docking simulations gave more accurate predictions than flexible docking simulations. The accuracy was also affected by both the simulation temperature and the kind of force field. The prediction rate of chiral preference was improved by as much as 76.7% when rigid-body MC docking simulations were performed at low-temperatures (100 K) with a sugar22 parameter set in the CHARMM force field. Our approach for MC docking simulations suggested that the conformational rigidity of both the host and guest molecule, due to either the low-temperature or rigid-body docking condition, contributed greatly to the prediction of chiral discrimination.

Key Words : Chiral discrimination, Conformational rigidity, Cyclodextrin, Grid-based Monte Carlo docking, Inclusion complex

Introduction

The separation of chiral compounds has been of great interest to researchers because the majority of biomolecules, such as proteins and carbohydrates, are chiral. In nature, these biomolecules only exist in one of the two possible enantiomeric forms, and living organisms show different biological responses to each pair of the enantiomers in drugs, pesticides, and waste compounds.[1] For effective chiral separation, numerous kinds of chiral stationary phases (CSP) or mobile phase additives have been developed since the 1960s. There are five categories of CSPs: Perkle, Cellulose, Inclusion complex, Ligand exchange, and Protein types.[2] Among these CSPs, cyclodextrins (CDs) and their derivatives are one of the most important inclusion complex forming agents in enantio-separation fields.[3] In the chiral recognition process, the enantiomers are identical and have the same size, the same shape, the same molecular electrostatics, etc.; therefore, they can only be distinguished when giving rise to slightly different diastereomeric responses upon associating with another chiral object or environment.[4] The intermolecular forces responsible for enantio-differentiation are the same as those in other cases of molecular recognition, but the differences of corresponding binding free energies are usually much smaller in magnitude. This is why enantio-selective prediction is so much more difficult than typical computational approaches.[5] Recently, numerous attempts to develop predictive models of enantio-selectivity

have been made with traditional molecular modeling strategies such as QSAR or neural network types.[6,7] However, these methods require developing scoring functions based on exact molecular descriptors for the chiral discrimination process. In contrast, force field-based calculations did not suffer from the necessity of exact molecular descriptors, although they do require many computational resources during simulations. These computing resource problems can be overcome by the use of high-performance computing equipment, such as the Grid system or parallel machines.[8]

In this research, we attempted to apply the Grid-based Monte Carlo (MC) docking simulations method to predict the chiral recognition between a guest enantiomer and the host CD at a molecular level. These force field-based calculations could be advantageous for analyzing molecular mechanisms as well as for effective conformational searching because these approaches can reproduce various ensembles for the enantio-selective conformations induced by the inclusion complexation.[9,10] Moreover, molecular simulations give us valuable insights on the physiological biomolecular conformations even though at high- or low- temperature.[11,12] In this study, either β-cyclodextrin (β-CD) or 6-amino-6-deoxy-β-cyclodextrin (am-β-CD) were used as hosts and 17 series of chiral compounds were used as guests, since these molecules were experimentally well-validated candidates for predicting the chiral preference.[13] MC docking simulations for chiral discrimination were performed using a CHARMM[14] program. The prediction of chiral preference was performed

based on binding free energy differences between each chiral guest and host cyclodextrin. The binding free energies are obtained using an ensemble average of trajectories extracted from these MC docking simulations. Such calculations require a very large amount of computing time on a single computer, which is impossible to handle in practice. In order to address this challenging computation requirement, we have developed a computational Grid system, called MGrid, to process a large number of force field calculations simultaneously. The MGrid system was designed to support remote execution, file transfers, and standard interface to legacy MPI (Message Passing Interface) applications to run successful MC docking simulations.

Results and Discussion

We define the chiral prediction rate as the percentage of correctly predicted preferences between R- and S-enantio-

mers in a total of 30 systems of chiral complexes. We tried to predict chiral preferences in one pair of enantio-complexes based on the MC docking simulations. Table 1 lists the binding free energy differences for chiral discrimination and the prediction rate in MC docking simulations based on conjugate gradient energy-minimization with a carbohydrate solution force field (CSFF). The experimental and calculated binding free energies were present at the same order of magnitude in most cases. The error ranges of absolute binding free energies in the calculated results were reasonable compared with the ones obtained from the general MM-PBSA (Molecular Mechanics/Possion-Boltzmann Surface Area) approach reported by others.[15,16] The binding free energies were calculated from two different docking approaches: rigid-body or flexible MC docking simulations. In rigid-body docking, the ligand enantiomers were regarded as rigid solid bodies, so just one conformer with the lowest-potential energy was evaluated for docking simulations.

Table 1. Binding free energies (kcal/mol) of inclusion complexes of chiral guests with β-CD or am-β-CD from MC docking simulations based on the flexible- or rigid-body docking

	Complex	Experiment				Flexible Docking[a]				Rigid-body Docking[a]			
		ΔG_R	ΔG_S	$\Delta\Delta G$	P_{obs}	ΔG_R	ΔG_S	$\Delta\Delta G$	P_{cal}	ΔG_R	ΔG_S	$\Delta\Delta G$	P_{cal}
1	N-t-Boc-alanine / β-CD	−3.54	−3.50	+0.04	R	−4.53	−3.98	+0.55	R	−6.99	−4.40	+2.59	R
2	N-t-Boc-alanine methyl ester / β-CD	−3.85	−3.77	+0.08	R	−11.39	−11.57	−0.18	S	−12.42	−11.12	+1.30	R
3	N-Cbz-alanine / β-CD	−2.96	−2.95	+0.01	R	1.59	−6.13	−7.72	S	−6.77	−6.60	+0.17	R
4	N-Cbz-aspartic acid / β-CD	−2.52	−2.55	−0.03	S	18.52	16.92	−1.60	S	9.75	18.50	+8.75	R
5	N-acetyl-phenylalanine / β-CD	−2.43	−2.49	−0.06	S	−3.99	−2.83	+1.16	R	−5.02	−5.42	−0.40	S
6	N-acetyl-tyrosine / β-CD	−2.85	−2.88	−0.03	S	−2.22	−7.06	−4.84	S	−3.12	−1.70	+1.42	R
7	N-acetyl-tryptophan / β-CD	−1.51	−1.68	−0.17	S	−6.86	−4.00	+2.86	R	−3.90	−3.18	+0.72	R
8	Gly-Phe / β-CD	−2.28	−2.36	−0.08	S	0.34	−7.09	−7.43	S	−3.25	−4.37	−1.12	S
9	mandelic acid / β-CD	−1.41	−1.29	+0.12	R	2.55	3.00	+0.45	R	2.51	2.52	0.01	−
10	mandelic acid methyl ester / β-CD	−2.49	−2.53	−0.04	S	−7.50	−7.32	+0.18	R	−6.99	−6.63	+0.36	R
11	hexahydromandelic acid / β-CD	−3.84	−3.79	+0.05	R	−1.87	−2.25	−0.38	S	−1.95	−1.59	+0.36	R
12	3-bromo-2-methyl-1-propanol / β-CD	−2.94	−2.93	+0.01	R	−7.39	−5.75	+1.64	R	−6.44	−6.13	+0.31	R
13	camphanic acid / β-CD	−3.07	−3.16	−0.09	S	−8.21	−11.45	−3.24	S	−10.70	−10.22	+0.48	R
14	camphorsulfonic acid / β-CD	−3.75	−3.67	+0.08	R	−7.46	−5.34	+2.12	R	−6.94	−4.96	+1.98	R
15	O,O'-toluoyl-tartaric acid / β-CD	−2.76	−2.70	+0.06	D	−1.69	1.85	+3.54	D	−1.90	−0.48	+1.42	D
16	O,O'-dibenzoyl-tartaric acid / β-CD	−2.06	−1.77	+0.29	D	−1.72	4.68	+6.4	D	−0.34	0.42	+0.76	D
17	N-t-Boc-alanine / am-β-CD	−3.88	−3.78	+0.10	R	−6.31	−5.70	+0.61	R	−5.69	−2.70	+2.99	R
18	N-t-Boc-alanine methyl ester / am-β-CD	−3.54	−3.47	+0.07	R	−10.33	−11.05	−0.72	S	−12.23	−12.06	+0.17	R
19	N-Cbz-alanine / am-β-CD	−3.09	−3.05	+0.04	R	−6.91	−6.60	+0.31	R	−3.58	−2.69	+0.89	R
20	N-acetyl-phenylalanine / am-β-CD	−2.41	−2.58	−0.17	S	−3.30	−2.66	+0.64	R	−1.99	−5.05	+3.06	R
21	N-acetyl-tyrosine / am-β-CD	−2.81	−2.90	−0.09	S	−1.52	−2.17	−0.65	S	−0.05	−1.15	−1.10	S
22	N-acetyl-tryptophan / am-β-CD	−1.63	−1.94	−0.31	S	−0.36	−0.52	−0.16	S	3.94	−1.52	−5.46	S
23	Gly-Phe / am-β-CD	−2.17	−2.21	−0.04	S	0.50	−0.54	−1.04	S	−4.26	−4.51	−0.25	S
24	mandelic acid / am-β-CD	−2.37	−2.25	+0.12	R	−1.84	3.47	+5.31	R	4.31	4.28	−0.03	S
25	hexahydromandelic acid / am-β-CD	−4.58	−4.33	+0.25	R	−0.61	−1.11	−0.50	S	−1.28	0.09	+1.37	R
26	1-cyclohexylethylamine / am-β-CD	−3.10	−3.12	−0.02	S	−0.63	2.08	+2.71	R	5.28	1.51	−3.77	S
27	3-bromo-2-methyl-1-propanol / am-β-CD	−2.81	−2.80	+0.01	R	−7.21	−7.50	−0.29	S	−6.34	−6.55	−0.21	S
28	camphanic acid / am-β-CD	−3.05	−3.16	−0.11	S	−10.11	−4.74	+5.37	R	−7.18	−7.38	−0.20	S
29	camphorsulfonic acid / am-β-CD	−3.95	−3.99	−0.04	S	−3.71	−5.14	−1.43	S	−7.09	−4.26	−2.83	R
30	O,O'-dibenzoyl-tartaric acid / am-β-CD	−2.45	−2.24	+0.21	D	4.90	11.75	−6.85	L	5.52	6.10	+0.58	D
	Prediction Rate (%)							56.7				66.7	

[a]conjugate-gradient energy-minimization method was used;

Flexible docking, on the other hand, allowed the evaluation for multiple conformers of ligands using dihedral angle rotations.[17] The backbone integrity of host CD molecules was maintained using a rigid harmonic constraint. The rigid-body MC docking simulations gave the prediction rate as 66.7%, while flexible docking showed a 56.7% accuracy at room temperature (298 K). The rigid-body docking method might be preferred to the flexible docking method for the accurate chiral discrimination process. This accuracy might originate from characteristics of the chiral recognition process, which is driven by rigid three-point interaction.[18,19] Based on those results, the rigid-body docking method combined with an energy-minimization method was adopted as a basic MC docking protocol for the prediction of chiral recognition by cyclodextrins.

We optimized an acceptance probability, which is defined as the ratio of accepted moves to trial moves during MC simulations. The acceptance probability is an important quantity for understanding the efficiency of MC simulations because the RMSD (root mean squared deviation) and displacements of each MC move are varied as a function of the acceptance probability.[20,21] These quantities should go to zero for a small acceptance probability, since most moves are rejected, and also for a high acceptance probability, since each trial move is too small.[22] Thus, acceptance probability is often adjusted during MC simulations so that about half of the trial moves are rejected.[23] The prediction rates for the acceptance probability of 0.1, 0.3, 0.5, and 0.7 in our Grid-based MC docking simulations were estimated to be 63.3, 60.0, 66.7, and 60.0%, respectively. The accuracy was lowered when the acceptance probability was either higher or lower than 0.5. Thus, an optimal acceptance probability of 0.5 was selected for our MC docking simulations for predicting chiral preference.

Table 2 shows the result of temperature on the prediction rate during the MC docking simulations. Criteria based both on interaction energy ($\Delta E_{interaction}$, data not shown) and binding free energy ($\Delta G_{binding}$, Table 2) were examined. In

Table 2. Binding free energies (kcal/mol) of inclusion complexes of chiral guests with β-CD or am-β-CD from MC docking simulations with different temperature using CSFF parameter set

Complex	Experiment	100 K			300 K			500 K			700 K		
	P_{obs}	ΔG_R	ΔG_S	P_{cal}	ΔG_R	ΔG_S	P_{cal}	ΔG_R	ΔG_S	P_{cal}	ΔG_R	ΔG_S	P_{cal}
1	R	−7.01	−3.94	R	−6.99	−4.40	R	−5.53	−2.55	R	−5.58	−2.93	R
2	R	−12.87	−10.76	R	−12.42	−11.12	R	−11.79	−11.79	−	−11.40	−11.43	S
3	R	−4.73	−5.55	S	−6.77	−6.60	R	−5.37	−6.63	S	−5.25	−5.51	S
4	S	10.22	19.97	R	9.75	18.50	R	12.81	20.24	R	19.37	19.59	R
5	S	−3.59	−4.82	S	−5.02	−5.42	S	−3.19	−4.40	S	−0.40	−1.90	S
6	S	−2.11	−0.08	R	−3.12	−1.70	R	−2.03	−2.35	S	−1.64	−0.69	R
7	S	−2.82	3.07	R	−3.90	−3.18	R	−0.34	−0.69	S	0.21	−0.13	S
8	S	−2.86	−3.60	S	−3.25	−4.37	S	0.16	−2.35	S	−2.74	0.01	R
9	R	−1.23	4.10	R	2.51	2.52	−	3.49	3.58	R	3.88	3.74	S
10	S	−8.78	−8.04	R	−6.99	−6.63	R	−5.85	−5.85	−	−11.84	−5.06	R
11	R	−0.50	−0.72	S	−1.95	−1.59	R	−1.33	−1.26	R	−0.91	−0.84	R
12	R	−8.76	−7.11	S	−6.44	−6.13	R	−5.37	−5.77	S	−4.69	−3.99	R
13	S	−11.61	−9.55	R	−10.70	−10.22	R	−8.67	−8.93	S	−8.46	−8.05	R
14	R	−6.28	−8.17	S	−6.94	−4.96	R	−4.27	−3.33	R	−4.37	−3.16	R
15	D	0.17	0.52	D	−1.90	−0.48	D	0.15	0.80	D	0.61	1.22	D
16	D	0.33	1.63	D	−0.34	0.42	D	1.50	2.19	D	2.10	2.66	D
17	R	−7.14	−2.06	R	−5.69	−2.70	R	−5.68	−2.74	R	−4.64	−0.86	R
18	R	−11.59	−12.31	S	−12.23	−12.06	R	−11.43	−12.50	S	−11.53	−11.51	R
19	R	−4.93	−5.54	S	−3.58	−2.69	R	−4.04	−5.59	S	−2.66	−2.34	R
20	S	−2.58	−6.15	S	−1.99	−5.05	R	−3.10	−5.42	S	−2.73	−3.13	S
21	S	−3.42	−1.74	R	−0.05	−1.15	S	−2.45	−1.74	R	−2.10	−1.70	R
22	S	1.20	−3.63	S	3.94	−1.52	S	2.56	0.78	S	1.45	0.56	S
23	S	−4.12	−4.51	S	−4.26	−4.51	S	−2.89	−2.58	R	−2.11	−1.94	R
24	R	2.34	2.65	R	4.31	4.28	S	3.39	3.44	R	2.97	3.52	R
25	R	−2.34	−1.69	R	−1.28	0.09	R	−1.19	−1.13	R	−1.00	−0.79	R
26	S	−8.31	5.41	R	5.28	1.51	S	4.39	5.22	R	5.41	6.16	R
27	R	−6.46	−4.72	R	−6.34	−6.55	S	−5.47	−4.80	R	−4.09	−4.29	S
28	S	−10.89	−8.50	R	−7.18	−7.38	S	−7.85	−8.12	S	−7.87	−7.76	R
29	S	−10.31	−11.17	S	−7.09	−4.26	R	−5.16	−4.34	R	−3.53	−2.04	R
30	D	2.31	4.10	D	5.52	6.10	D	3.16	4.35	D	3.43	4.55	D
Prediction Rate (%)		50.0			66.7			63.3			53.3		

Table 3. Binding free energies (kcal/mol) of inclusion complexes of chiral guests with β-CD or am-β-CD from MC docking simulations with different temperature using sugar22 parameter set

Complex	Experiment	100 K			300 K			500 K			700 K		
	P_{obs}	ΔG_R	ΔG_S	P_{cal}	ΔG_R	ΔG_S	P_{cal}	ΔG_R	ΔG_S	P_{cal}	ΔG_R	ΔG_S	P_{cal}
1	R	−8.32	−7.64	*R*	−7.86	−3.84	*R*	−7.39	−4.93	*R*	−7.15	−3.69	*R*
2	R	−10.90	−12.13	S	−10.78	−11.42	S	−10.90	−10.24	R	−9.89	−9.46	R
3	R	−9.10	−8.87	*R*	−8.32	−8.95	S	−7.39	−7.95	S	−7.04	−7.57	S
4	S	3.30	3.72	R	4.42	4.60	R	5.54	12.10	R	14.01	12.08	R
5	S	−5.63	−7.03	*S*	−5.53	−6.10	*S*	−4.79	−5.91	*S*	−4.11	−4.98	*S*
6	S	−3.33	−5.19	*S*	−3.24	−3.10	R	−3.05	−4.55	*S*	−3.16	−4.06	*S*
7	S	−1.42	−1.78	*S*	−1.82	−1.78	R	−1.20	−0.97	R	0.02	−1.04	*S*
8	S	6.81	7.43	R	6.35	6.72	R	5.95	7.93	R	6.92	7.49	R
9	R	0.57	1.04	*R*	0.23	0.40	*R*	0.53	0.77	*R*	1.01	1.07	*R*
10	S	−6.02	−6.27	*S*	−4.74	−4.90	*S*	−4.65	−4.49	R	−3.39	−3.68	*S*
11	R	−4.27	−4.20	*R*	−4.21	−4.15	*R*	−3.89	−3.95	S	−3.50	−3.45	*R*
12	R	−5.52	−5.17	*R*	−4.62	−4.20	*R*	−4.34	−4.15	*R*	−5.09	−5.14	S
13	S	−13.71	−12.74	R	−12.84	−12.00	R	−11.52	−11.52	−	−11.11	−10.66	R
14	R	−11.51	−10.39	*R*	−9.36	−7.85	*R*	−8.57	−6.93	*R*	−8.14	−6.66	*R*
15	D	−11.84	−10.54	*D*	−11.50	−10.55	*D*	−10.57	−10.38	*D*	−10.69	−10.16	*D*
16	D	−10.10	−10.08	*D*	−10.43	−9.89	*D*	−9.96	−9.29	*D*	−9.54	−9.34	*D*
17	R	−7.34	−4.32	*R*	−6.92	−4.15	*R*	−6.41	−3.38	*R*	−5.65	−3.09	*R*
18	R	−12.14	−9.85	*R*	−10.34	−10.63	S	−10.07	−9.28	*R*	−8.33	−8.72	S
19	R	−4.63	−4.20	*R*	−6.47	−7.66	S	−5.54	−7.03	S	−5.25	−6.50	S
20	S	−4.42	−8.07	*S*	−5.58	−7.57	*S*	−5.05	−6.88	*S*	−3.92	−5.87	*S*
21	S	−3.95	−5.99	*S*	−5.17	−4.61	R	−3.87	−4.25	*S*	−3.29	−3.60	*S*
22	S	−0.72	−4.18	*S*	−2.41	−2.25	R	−2.21	−1.70	R	−2.19	−1.51	R
23	S	−3.02	−3.31	*S*	−1.84	−2.32	S	−1.61	−1.25	R	−0.38	−0.85	*S*
24	R	0.05	0.27	*R*	0.01	0.42	*R*	0.67	0.95	*R*	1.49	1.56	*R*
25	R	−5.21	−4.71	*R*	−4.57	−4.26	*R*	−4.03	−3.56	*R*	−3.07	−2.88	*R*
26	S	4.31	7.52	R	1.44	5.04	R	4.25	6.01	R	4.35	4.94	R
27	R	−4.80	−6.88	S	−3.91	−2.56	*R*	−3.75	−2.01	*R*	−4.74	−1.60	*R*
28	S	−11.75	−10.97	R	−11.16	−10.82	R	−10.63	−10.30	R	−9.62	−9.82	*S*
29	S	−12.14	−12.16	*S*	−9.42	−8.98	R	−7.29	−6.95	R	−6.57	−5.42	R
30	D	−7.71	−6.90	*D*	−7.35	−6.88	*D*	−6.98	−6.35	*D*	−6.79	−6.15	*D*
Prediction Rate (%)		76.7			50.0			56.7			66.7		

the interaction energy-based prediction, a maximum accuracy of 63.7% was obtained with 700 K of high simulation temperature (data not shown). In the chiral prediction based on binding free energy, a maximum prediction rate of 66.7% was obtained at a temperature of 300 K, where binding free energy was calculated from interaction energy with solvation energy terms. Hard calculations for solvation energy terms did not affect the prediction rate at any temperature on the carbohydrate solution force field (CSFF). Since the prediction rate was not optimized by adjusting the simulation temperature, the CSFF parameter set used in MC simulations was changed to a sugar22 parameter as an alternative carbohydrate force field developed for CHARMM. The sugar22 parameter set used in CHARMM normally supports the increased force constant in the hydroxymethyl dihedral angle (O5-C5-C6-O6), in contrast to the CSFF parameter. We then examined the temperature effect on the prediction rate based on interaction energy criterion (data not shown) and binding free energy criterion (Table 3) with this sugar22

parameter set. In chiral prediction based on interaction energy, the prediction rate reached a range of 50.0-56.7% without being significantly affected by temperature. However, the accuracy increased to as high as 76.7% in the binding free energy-based prediction for rigid-body MC docking simulations at 100 K. This result suggests that the prediction of chiral discrimination could be optimized at low-temperatures with solvation contribution.

According to the accepted theory for chiral recognition, three simultaneous interactions between the chiral stationary phase (CSP) and at least one of the chiral guests are required, and one of these interactions must be stereochemically dependent.[2,19] Cyclodextrins can distinguish enantiomers by the presence or absence of a third intermolecular interaction.[24,25] Therefore, it is expected that the conformationally rigid CSP interacts strongly with the guest compound in the chiral recognition process. At lower temperatures, a large portion of high-energy structures are rejected while a few are accepted during the Metropolis MC

docking simulations. Therefore, the low-temperature simulations with rigid-body docking conditions might increase the conformational rigidity of both host and guest to enhance the chiral recognition process.

Our MC docking simulations method revealed that the conformational rigidity of both the host and guest plays a key role in chiral discrimination predicting since the rigid-body docking and low-temperature condition with the sugar22 parameter set resulted in the most accurate prediction of chiral preference. The CSFF is a specially designed parameter set to describe the correct hydroxymethyl conformer distribution of glucopyranose residue in water by decreasing the force constant in the hydroxymethyl dihedral angle (O5-C5-C6-O6).[26] That decrease in the dihedral parameters acts as an incentive to more flexible conformational behavior of cyclodextrins during MC docking simulations based on the CSFF parameter. This reduction of steric hindrance could cause increased ambiguity[18] in the computational prediction of chiral discrimination based on force field calculation. That is why CSFF is less accurate than the sugar22 parameter set.

The reduced conformational flexibility in the rigid-body and low-temperature model in our simulation method was effective for the maximization of *in silico* chiral discrimination. Our results suggest that use of the rigid molecular model may be advantageous to the computational chiral prediction. In this respect, the optimization of computational parameters for molecular docking simulations would be highly recommended in the context of a rigid molecular model considering solvation effect for the accurate prediction of chiral discrimination.

Methods of Computation

Construction of the molecular models and protocol of MC docking simulations. The starting configuration of the β-CD for MC simulations was taken from an X-ray crystal structure, and the am-β-CD was prepared by amino-deoxy modification for template β-CD using the InsightII/Builder module (version 2000, Accelrys Inc. San Diego, USA). The missing hydrogen atoms in the X-ray coordinates were built with the InsightII program. The 17 series of chiral guest molecules were built with the InsightII/Biopolymer module. The initial conformations of each chiral guest were determined using simulated annealing molecular dynamics (SA-MD) simulations for geometry optimization. All simulations were performed using a general molecular modeling program, CHARMM (version 28b2), with a parm22 all-atom force field. In SA-MD simulations, the temperature was alternated between 300 and 1000 K ten times. The total time for SA-MD simulation was 3,000 ps. Ten structures were saved and fully energy-minimized at the end of each production phase at 300 K, and the lowest-energy conformation among the ten structures was selected for the initial structure of the next SA-MD cycle. The starting configurations of guest compounds for the MC docking simulations were taken from the SA-MD conformations with the lowest-
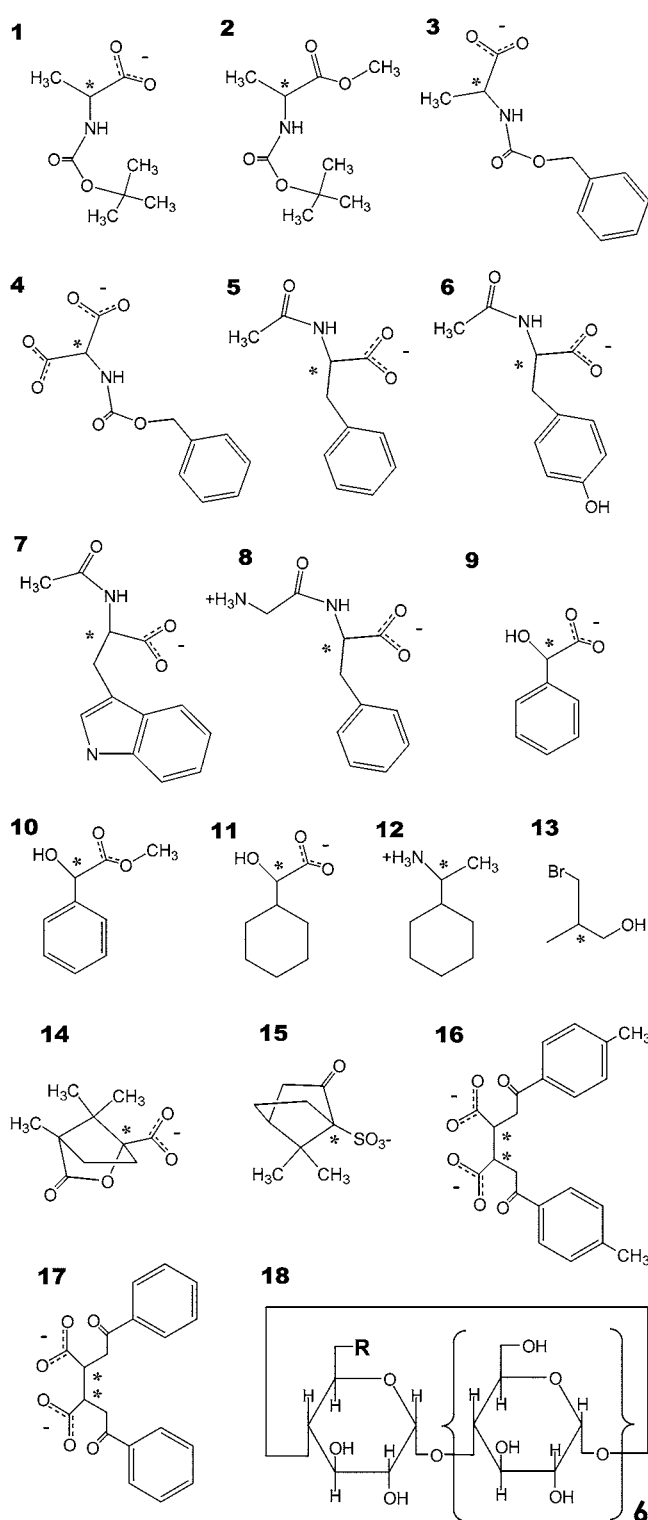

Figure 1. Chiral guests and host cyclodextrins considered in this work: **1**. *N-t*-Boc-alanine; **2**. *N-t*-Boc-alanine methyl ester; **3**. *N*-Cbz-alanine; **4**. *N*-Cbz-aspartic acid; **5**. *N*-acetyl-phenylalanine; **6**. *N*-acetyl-tyrosine; **7**. *N*-acetyl-tryptophan; **8**. Gly-Phe; **9**. mandelic acid; **10**. mandelic acid methyl ester; **11**. hexa-hydromandelic acid; **12**. 1-cyclohexylethylamine; **13**. 3-bromo-2-methyl-1-propanol; **14**. camphanic acid; **15**. camphorsulfonic acid; **16**. *O,O'*-toluoyl-tartaric acid; **17**. *O,O'*-dibenzoyl-tartaric acid; **18**. β-cyclodextrin (R = OH) and 6-amino-6-deoxy-β-cyclodextrin (R = NH_3^+).

energy value. Their two-dimensional molecular structures are depicted in Figure 1. The MC docking simulations were performed using a "MC" module of CHARMM. The parameter values for the β-CD were modified according to a revised carbohydrate parameter set (carbohydrate solution force field or sugar22 force field) of the CHARMM. The short-range nonbonded interactions were truncated with a 13-Å cutoff. An implicit solvent water model was used with a distance-dependent dielectric constant (3r). The docking process was assumed to be a 1 : 1 interaction between each host and chiral guest during the MC runs. The initial configuration of each host and guest molecule was positioned arbitrarily within a neighboring distance. Trials to a new configuration were accomplished by changing each move set of a guest molecule. The MC move set for flexible docking was composed of rigid translations, rigid rotations, and rotations of freely rotatable dihedral angles of the guest. For rigid-body docking, dihedral rotations of the MC move set were interrupted. A single step consists of picking a random conformer, making a random move, minimizing the energy of a new conformer, and then checking the energy with a Metropolis[27] criterion. This process uses a combined methodology consisting of Metropolis criterion for a global optimization and an energy minimization method for a local optimization.[28] Host CDs were weakly fixed using a harmonic positional restraint of CHARMM to maintain backbone integrity. The MC-minimized structures were saved every 20 steps for 20,000 trials. These MC processes produced various docked structures for each host with its chiral guest.

Binding free energy calculation methods. The MM-PBSA methodology,[29] which was originally developed for molecular dynamics simulations by P. A. Kollman *et al.*, was applied to the analysis of our MC trajectories. The method estimates the free energies of binding by combining the absolute energies in the gas phase (E_{MM}), solvation free energies ($G_{PB} + G_{nonpolar}$), and entropy changes (TS) for each guest, host, and complex. The interaction energy and the difference of binding free energy between the R-enantiomer and S-enantiomer complexes are defined as:

$$\Delta\Delta G_{binding} = \Delta G_S - \Delta G_R \tag{1}$$

$$\Delta G_{binding} = \Delta G_{(complex)} - [\Delta G_{(host)} + \Delta G_{(guest)}] \tag{2}$$

$$G_{molecule} = <E_{MM}> + <G_{PB}> + <G_{nonpolar}> - TS \tag{3}$$

$$E_{MM} = E_{vdw} + E_{elec} \tag{4}$$

$$\Delta E_{interaction} = \Delta E_{(complex)} - [\Delta E_{(host)} + \Delta E_{(guest)}] \tag{5}$$

where < > denotes an average over a set of snapshots along an MC trajectory. E_{vdw} and E_{elec} denote van der Waals and electrostatic energies, respectively. The polar contribution to the solvation free energy (G_{PB}) was calculated by solving the Poisson–Boltzmann equation with the "PBEQ" module of the CHARMM program. For the PBEQ calculations, the grid spacing was set at 0.5 Å, the molecule was filled with the grid box, and 2,000 iterations were performed to ensure

the maximum change in potential was less than 2×10^{-6} kT/e. The dielectric constant inside and outside the molecule was 1.0 and 80.0, respectively. The nonpolar solvation contribution includes cavity creation in water and vdW interactions between the modeled nonpolar molecule and water molecules. This term can be imagined as transferring a nonpolar molecule with the shape of the host or guest from vacuum to water. This transfer of free energy is described as[30]: $\Delta G_{nonpolar} = \gamma A + b$, where A is the solvent-accessible surface area calculated by the CHARMM program, and γ and b are 0.00542 kcal/mol·Å² and 0.92 kcal/mol, respectively, derived from the experimental transfer energies of hydrocarbons.[31] The probe radius was 1.4 Å. In eq. (3), S is the entropy change for the host-guest complexation. The solvent entropy changes caused by polarization and cavity formation are included in the polar and nonpolar solvation-free energy terms. The solute entropy changes are almost identical because the structural properties of each are identical in enantiomers. Thus, in this study the entropy change of each enantiomeric complex upon binding is assumed to be equal.[32,33]

Molecular Grid system (MGrid). In addition to the development of these novel simulation techniques for the prediction of chiral discrimination, we have also constructed a computational Grid system called MGrid.[34] This computing system is motivated by the large number of required force field calculations that are, in practice, impossible to handle with a single computer. The MGrid system is designed to allow us to execute a number of simulation jobs on remote computers simultaneously and to examine the results in a user-friendly Web-based problem-solving environment. In addition, MGrid automatically stores these simulation results in databases for later retrieval and supports various searching methods. A prototype system was installed and implemented on Konkuk University's Linux cluster, which has 30 nodes with dual Xeon 2.0 GHz CPUs. We used the MGrid system to run the entire MC simulation on a number of computers simultaneously and, as a result, were able to reduce simulation time significantly. The MGrid system also helped us manage a number of jobs and their results in a simple and secure manner via an easy-to-use Web-based user interface. With this Linux cluster, it took about 15,000 hours to produce the simulation results presented in this paper. Currently, the MGrid system is being ported to the testbed (http://testbed.gridcenter.or.kr/eng/), which is a cluster of Linux clusters and supercomputers at a number of universities and research institutes. Once this porting is finished, the MGrid system will be able to provide much more computing power and will allow us to tackle more challenging problems.

Dinner, A. R. for the helpful discussion on the MC docking during preparation of the manuscript. SDG.

References

1. Cabusas, M. E. *Ph. D. Thesis*; Virginia Polytechnic Institute and State University: USA, 1998; pp 1-9.
2. Pirkle, W. H.; Pochapsky, T. C. *Chem. Rev.* **1989**, *89*, 347.
3. Lee, S.; Yi, D. H.; Jung, S. *Bull. Korean Chem. Soc.* **2004**, *25*, 216.
4. Lipkowitz, K. B.; Coner, R.; Peterson, M. A. *J. Am. Chem. Soc.* **1997**, *119*, 11269.
5. Dodziuk, H.; Lukin, O. *Chem. Phys. Lett.* **2000**, *327*, 18.
6. Wolbach, J. P.; Lloyd, D. K.; Wainer, I. W. *J. Chromatogr. A* **2001**, *914*, 299.
7. Booth, T. D.; Azzaoui, K.; Wainer, I. W. *Anal. Chem.* **1997**, *69*, 3879.
8. Natrajan, A.; Crowley, M.; Wilkins, N.; Humphrey, M. A.; Fox, A. D.; Grimshaw, A. S.; Brooks, C. L. III *High Perform. Distribu. Compu.* **2001**, *10*, 1.
9. Ferguson, D. M.; Raber, D. J. *J. Am. Chem. Soc.* **1989**, *111*, 4371.
10. Choi, Y. H.; Yang, C. H.; Kim, H. W.; Jung, S. *Carbohydr. Res.* **2000**, *328*, 393.
11. Lee, J.; Jang, S.; Pak, Y.; Shin, S. *Bull. Korean Chem. Soc.* **2003**, *24*, 785.
12. Bouzida, D.; Rejto, P. A.; Verkhivker, G. M. *Int. J. Quant. Chem.* **1999**, *73*, 113.
13. Rekharsky, M. V.; Inoue, Y. *J. Am. Chem. Soc.* **2002**, *124*, 813.
14. Brooks, B. R.; Bruccoleri, R. E.; Olafson, B. D.; States, D. J.; Swaminathan, S.; Karplus, M. *J. Comput. Chem.* **1983**, *4*, 187.
15. Wang, W.; Lim, W. A.; Jakalian, A.; Wang, J.; Wang, J.; Luo, R.; Bayly, C. I.; Kollman, P. A. *J. Am. Chem. Soc.* **2001**, *123*, 3986.
16. Bea, I.; Jaime, C.; Kollman, P. A. *Theor. Chem. Acc.* **2002**, *108*, 286.
17. Halperin, I.; Ma, B.; Wolfson, H.; Nussinov, R. *Proteins* **2002**, *47*, 409.
18. Ahn, S.; Ramirez, J.; Grigorean, G.; Lebrilla, C. B. *J. Am. Soc. Mass Spec.* **2001**, *12*, 278.
19. Kano, K. *J. Phys. Org. Chem.* **1997**, *10*, 286.
20. Fletcher, R.; Reeves, C. M. *Compu. J.* **1964**, *7*, 149.
21. Mbamala, E. C.; Pastore, G. *Phys. A* **2002**, *313*, 312.
22. Bouzida, D.; Kumar, S.; Swendsen, R. H. *Phys. Rev. A* **1992**, *45*, 8894.
23. Allen, M. P.; Tildesley, D. J. *Computer Simulations of Liquids*; Oxford University Press: New York, 1987.
24. Jung, E.; Jeong, K.; Lee, S.; Kim, J.; Jung, S. *Bull. Korean Chem. Soc.* **2003**, *24*, 1627.
25. Kim, H.; Jeong, K.; Lee, S.; Jung, S. *Bull. Korean Chem. Soc.* **2003**, *24*, 95.
26. Kuttel, M.; Brady, J. W.; Naidoo, K. J. *J. Comput. Chem.* **2002**, *23*, 1236.
27. Metropolis, N.; Rosenbluth, A. W.; Rosenbluth, M. N.; Teller, A. H.; Teller, E. *J. Chem. Phys.* **1953**, *21*, 1087.
28. Caflisch, A.; Fischer, S.; Karplus, M. *J. Comput. Chem.* **1997**, *18*, 723.
29. Srinivasan, J.; Cheatham, T. E.; Cieplak, P.; Kollman, P. A.; Case, D. A. *J. Am. Chem. Soc.* **1998**, *120*, 9401.
30. Sitkoff, D.; Sharp, K. A.; Honig, B. *J. Phys. Chem.* **1994**, *98*, 1978.
31. Kirschner, K. N.; Woods, R. J. *Proc. Natl. Acad. Sci. U.S.A.* **2001**, *98*, 10541.
32. Huo, S.; Massova, I.; Kollman, P. A. *J. Comput. Chem.* **2002**, *23*, 15.
33. Choi, Y.; Jung, S. *Carbohydr. Res.* **2004**, *339*, 1961.
34. Jeong, K.; Kim, D.; Kim, M.; Hwang, S.; Jung, S.; Lim, Y.; Lee, S. *Lecture Notes in Computer Science* **2003**, *2660*, 1117.